Electrochemical Tuning of Electronic Structure of C_{60} and C_{70} Fullerene Peapods: In Situ Visible Near-Infrared and Raman Study

Ladislav Kavan,*,†,‡ Lothar Dunsch,‡ Hiromichi Kataura,§ Atsushi Oshiyama,|| Minoru Otani,|| and Susumu Okada||

J. Heyrovský Institute of Physical Chemistry, Academy of Sciences of the Czech Republic, Dolejškova 3, CZ-182 23 Prague 8, Czech Republic, Institute of Solid State and Materials Research, Helmholtzstrasse 20, D-01069 Dresden, Germany, Department of Physics, Tokyo Metropolitan University, 1-1 Minami-Ohsawa, Hachioji, Tokyo 192-0397, Japan, and Institute of Physics, University of Tsukuba, Tsukuba, Ibaraki 305-8571, Japan

Received: May 14, 2003

The population of valence-band electronic states of fullerene peapods (C_{60}@SWCNT and C_{70}@SWCNT) was tuned electrochemically in 0.2 M $LiClO_4$ + acetonitrile. Electrochemistry of peapods is dominated by their capacitive charging without distinct faradaic processes. In situ vis-NIR spectra of C_{60}/C_{70} peapods are similar to those of empty nanotubes. Electrochemical charging causes reversible bleaching of the transitions between Van Hove singularities. This bleaching is mirrored by quenching of resonance Raman spectra in the regions of tube-related modes. The Raman modes of intratubular C_{60} exhibit considerable intensity increase upon anodic doping of peapods, but these Raman modes are not enhanced at cathodic charging. In contrast to that, C_{70}@SWCNT does not show any enhancement of Raman intensities at both anodic and cathodic potentials. All the relevant Raman modes of intratubular C_{70} show symmetric charge-transfer bleaching as the tube-related modes. A suggested interpretation follows from model calculations of electronic structure of C_{70}@SWCNT (17,0) and C_{60}@SWCNT (17,0).

1. Introduction

Fullerenes C_{60} and C_{70} exhibit similar electrochemistry in solution: both molecules are cathodically reduced in acetonitrile−toluene mixtures in six reversible one-electron steps, which occur between −0.97 and −3.26 V vs Fc/Fc^+ (Fc = ferrocene).[1] Electrochemical reduction of thin solid films of C_{60}/C_{70} is irreversible,[2,3] and it is accompanied by a structural reconstruction.[2,3] The reductively driven reconstruction of the film morphology may even lead to formation of regular clusters of C_{60},[3] but no corresponding data on C_{70} films exist. Electrochemistry of single-walled carbon nanotubes (SWCNT) is dominated by double-layer charging with small contribution (if any) of faradaic pseudocapacitance of surface oxides.[4,5]

The discovery of fullerene peapods such as C_{60}@SWCNT[6] opened new routes to electrochemistry of carbon materials as both the host and the guest are redox-active. Recently, peapods with 85% filling for C_{60} and 72% for C_{70} were prepared.[7] The filling factor was determined from X-ray diffraction[7] and electron energy loss spectroscopy.[7,8] The C_{60} molecules in peapods represent a 1D crystal with a lattice constant of 0.977−0.95 nm, which is smaller than that in ordinary cubic C_{60} crystal (1.00 nm).[7] Because of the nonspherical symmetry of C_{70}, the 1D crystals of C_{70} in peapods show two different lattice constants, 1.00 and 1.10 nm, which were assigned to two "allotropic" 1D phases with different stacking density, equivalent to "standing" and "lying" cages of C_{70}.[7]

Nonaqueous electrochemistry of solid nanocarbons such as SWCNT allows easy and precise control of the population of electronic states near the Fermi level.[4] As both of the components of peapods, i.e., SWCNT and C_{60}/C_{70}, show specific redox response, there is a clear challenge to explore the behavior of peapods, addressing fundamental problems of electronic and redox properties of carbon nanostructures. The vis-NIR spectroelectrochemistry of empty SWNCT at varying potential points at reversible and fast bleaching of the electronic transitions between Van Hove singularities.[4] The bleaching causes reversible quenching of resonance Raman scattering of both radial breathing (RBM) and tangential (TM) modes of SWCNT.[4,9]

The Raman spectra of C_{60}/C_{70} peapods display, in general, the superposition of lines of the parent fullerenes and SWCNT, while the latter dominate the spectrum, especially at room temperature.[7,10,11] The free C_{60} molecule (I_h symmetry group) has 10 Raman-active vibrations ($2A_g + 8H_g$).[12,13] The vibrational structure of C_{70} is much more complex: the free molecule (D_{5h} symmetry group) has 53 Raman-active vibrations ($12A_1' + 22E_2' + 19E_1''$),[13,14] whose complete assignment is still a subject of debate.[13] For the excitations around 2.5 eV, the C_{60} features are resonance-enhanced via the first allowed transition in C_{60} ($h_u \rightarrow t_{1u}, t_{1g}$).[12] Also the C_{70} features are resonance-enhanced around 2.5 eV via several electronic transitions, which have been identified in this region.[14]

The C_{60} peapods are reducible by potassium vapor, forming a polymeric chain $(C_{60}^{6-})_n$ inside the SWNCT exhibiting metallic conductivity.[10] The coupled doping and polymerization by potassium allows the acquisition of Raman spectra at low temperatures (4−20 K), but the control of the doping level is, in principle, difficult.[10] Electrochemistry offers more favorable conditions for both reductive and oxidative doping, although it

* Corresponding author: e-mail kavan@jh-inst.cas.cz.
† Academy of Sciences of the Czech Republic.
‡ Institute of Solid State and Materials Research.
§ Tokyo Metropolitan University.
|| University of Tsukuba.

10.1021/jp035332f CCC: $25.00
Published on Web 07/04/2003

cannot be carried out in situ at very low temperatures. This paper is concerned with the electrochemical doping of peapods, which is, especially for the hole doping, superior to chemical redox doping. Our previous short communication[15] focused on electrochemical doping of C_{60}@SWCNT. Here we present new results on a detailed spectroelectrochemical study of C_{60}@SWCNT and C_{70}@SWCNT.

2. Experimental Section

Fullerene peapods (C_{60}@SWCNT, filling ratio 85% and C_{70}@SWCNT, filling ratio 72%) were prepared and purified as described elsewhere.[7,11] A thin film electrode was obtained by evaporation of freshly sonicated ethanolic slurry of peapods on Pt or ITO (indium−tin oxide conducting glass) sheets. The film was outgassed at 100−150 °C in a vacuum and further handled under nitrogen atmosphere. Electrochemical experiments were carried out on PG 300 (HEKA) or 273A (EG&G PAR) potentiostats with Pt auxiliary and Ag wire pseudoreference electrodes. The electrolyte solution was 0.2 M $LiClO_4$ in acetonitrile (both from Aldrich) dried by 4 Å molecular sieve (Union Carbide). The water content in the electrolyte solution was about 10 ppm (Karl Fischer titration). The electrolyte solution was purged with nitrogen, and the cell was assembled in a glovebox (M. Braun). The box atmosphere was N_2 containing <1 ppm O_2 and H_2O. For in situ Raman measurements, the cell was equipped with a glass optical window.

The ITO-supported film of peapods served as working electrode for in situ vis-NIR spectroelectrochemistry in 0.2 M $LiClO_4$ + acetonitrile. The spectra were recorded on a double-beam Shimadzu 3100 spectrometer. The working electrode was placed in a closed 2-mm optical cell with Pt auxiliary and Ag-wire pseudoreference electrodes. Optical densities were normalized against a second optical cell with blank ITO electrode. Due to limited stability of ITO against reductive breakdown, the vis-NIR spectra were studied at potentials >−0.9 V vs Fc/Fc^+.

Raman spectra were excited by Ar^+ laser at 2.41 or 2.54 eV, respectively (Innova 305, Coherent). The Raman spectra were recorded on a T-64000 spectrometer (Instruments, SA) interfaced to an Olympus BH2 microscope (objective 50×; the laser power impinging on the cell window was 1.6−1.7 mW). The spectrometer was calibrated before each series of measurements by using the F_{1g} mode of Si at 520.2 cm^{-1}. A second calibration was carried out by using the Raman bands of acetonitrile as an internal standard.[4] Along with the peapods, the parent empty SWCNTs were also studied by the same methods at identical conditions. The acquisition of each complete Raman spectrum took approximately 1 h. The potential of Ag wire pseudoreference electrode was calibrated against the redox potential of ferrocene, which was deliberately added to the electrolyte solution at the end of each set of spectro/electrochemical measurements. The actual fluctuations of Ag wire potential were of the order of 0.01 V during several weeks. The pseudoreference data were recalculated, and all potentials in this work were referred to the Fc/Fc^+ reference electrode.

3. Results and Discussion

3.1. Cyclic Voltammetry. Figure 1 displays a typical cyclic voltammogram of C_{70} peapods in 0.2 M $LiClO_4$ + acetonitrile. The voltammogram resembles that of C_{60}@SWCNT:[15] the plot is dominated by capacitive double-layer charging, analogous to that of empty SWCNT.[4,5] In analogy to C_{60}@SWCNT,[15] there are no distinct redox couples of C_{70}, although we would expect two C_{70}-related reduction waves at −0.97 and −1.34 V for molecular C_{70} (see arrows in Figure 1).[1] The capacitance of

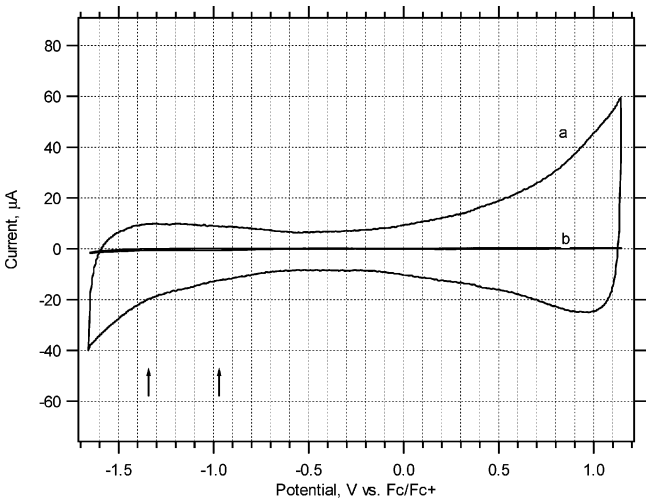

Figure 1. Cyclic voltammogram of C_{70}@SWCNT peapods deposited on a Pt electrode in 0.2 M $LiClO_4$ + acetonitrile; scan rate 0.1 V/s (curve a). Also shown is the voltammogram of blank Pt electrode at the same conditions (curve b). Arrows indicate the expected formal potentials corresponding to C_{70}/C_{70}^- and C_{70}^-/C_{70}^{2-} redox couples.

empty SWCNT was ca. 40 F/g in 0.2 M $LiClO_4$ + acetonitrile.[4] For an ideal double-layer capacitor, the change in the number of electrons transferred per one carbon atom, Δf equals

$$\Delta f = M_C C \Delta U / F \qquad (1)$$

where M_C is atomic weight of carbon, ΔU is potential difference, and F is Faraday constant. Equation 1 yields $\Delta f = 0.005$ e^-/C atom for $\Delta U = 1$ V and $C = 40$ F/g. A one electron reduction of C_{70} represents $\Delta f = 0.014$ e^-/C atom. Assuming the filling ratio of 72%,[7] the redox process C_{70}/C_{70}^- would correspond to about 2 times more electrons per C atom compared to the double layer charging of the wall. The absence of any distinct faradaic process evidences that the electroreduction of intratubular C_{70} is hampered. This is in accord with our earlier data on C_{60}@SWCNT[15] as well as with the fact that even a stronger chemical reduction of C_{60}@SWCNT with potassium vapor was sluggish, starting with a charge transfer to the nanotube wall.[10] The reduction of intratubular C_{60} up to $(C_{60}^{6-})_n$ required heavy doping by potassium.[10] Strong coulomb forces might hinder the electrochemical reduction of the inserted fullerene, as the extra electrons on C_{60}/C_{70} need to be compensated by solvated Li^+ cations, which may not penetrate into the peapod. Thus, the charge compensation "through-wall" is not sufficient, due to a limited double-layer capacity (cf. eq 1), and there would be a negatively charged fullerene row in a negatively charged nanotube mantle. Therefore, the C_{60}/C_{70} reduction is obviously suppressed in peapods.

3.2. Vis-NIR Spectroscopy. Figure 2 shows the vis-NIR spectra of dry films of peapods in air and the parent empty SWCNTs deposited on quartz substrates. All spectra are dominated by three characteristic absorptions at about 0.7, 1.25, and 1.8 eV, which can be attributed to electronic transitions between Van Hove singularities.[4,16] The first two transitions are assigned to singularities in semiconducting tubes ($\upsilon_s^1 \rightarrow c_s^1$) and ($\upsilon_s^2 \rightarrow c_s^2$), respectively, whereas the band at 1.8 eV corresponds to the first pair of singularities in metallic tubes ($\upsilon_m^1 \rightarrow c_m^1$).[4,16,17] Supposing that the transition energies scale with peapod diameters as in the case of empty tubes,[17−20] we can estimate the corresponding diameters to be close to 1.3 nm. Previous experimental[6,21,22] and theoretical[23] studies have shown that this is the optimum diameter of SWCNT to encapsulate

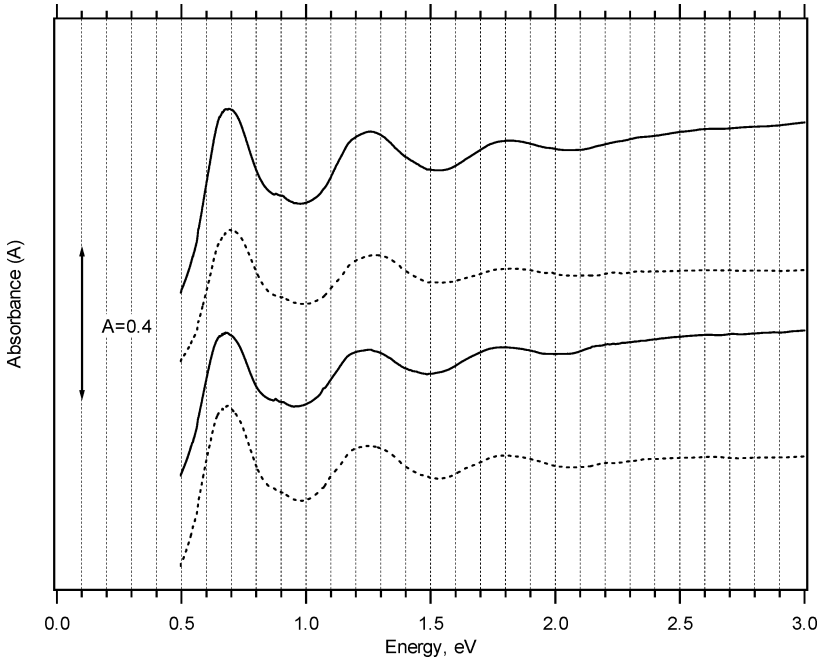

Figure 2. Vis-NIR spectra of dry films of peapods deposited on quartz substrate. From top to bottom: C_{60}@SWCNT, SWCNT (parent empty tubes for C_{60}@SWCNT), C_{70}@SWCNT, and SWCNT (parent empty tubes for C_{70}@SWCNT).

C_{60}. Apparently, the preferred structure exhibits the "graphite-like" distance (0.3 nm) between C_{60} and the tube wall.[6,22] No distinct optical transitions of C_{60}/C_{70} (expected at ca. 2.3−2.6 eV) are detected (Figure 2).

A careful inspection of Figure 2 reveals a small red shift of the optical transitions of peapods compared to those of empty tubes, both for C_{60} and C_{70} peapods. Second, a small red shift is expressed also by comparing the spectrum of C_{70}@SWCNT vs that of C_{60}@SWCNT (Figure 2). This points at two obvious conclusions: (i) Encapsulation of fullerene C_{60}/C_{70} causes some "swelling" of the tubes. (ii) The diameter of C_{70}@SWCNT is slightly larger than that of C_{60}@SWCNT. On the basis of optical and EELS spectra, Ijima et al. [8] have reported a similar red shift (14−25 meV) in C_{60}@SWCNT (compared to empty SWCNT), which corresponds to a diameter increase of 0.03 nm due to the C_{60} encapsulation. The diameter increase in the series empty tubes < C_{60}@SWCNT < C_{70}@SWCNT is also mirrored by the RBM in Raman spectra (see section 3.3).

Figure 3 panels A and B show the vis-NIR spectra of C_{60}@SWCNT and C_{70}@SWCNT, respectively, in contact with the electrolyte solution. The spectra at open-circuit potential (around −0.3 to 0 V vs Fc/Fc^+) are similar to those of dry films in air (Figure 2) except for noise introduced in the NIR region by strong absorptions of ITO, acetonitrile, and trace water. Electrochemical charging causes reversible disappearance of the electronic transitions, similar to that in empty SWCNT.[4,16,24,25] Anodic polarization shifts the Fermi level, while the corresponding singularities are depleted in the sequence υ_s^1, υ_s^2, υ_m^1. Analogously, cathodic polarization leads to sequential filling of the singularities: c_s^1, c_s^2, c_m^1. In both cases, the optical bands disappear in the same sequence. The NIR peak absorbance was found to be constant (±5%) at potentials inside the $\upsilon_s^1-c_s^1$ gap but decreased symmetrically at larger/smaller potentials outside the gap.[16]

Nevertheless, the complete bleaching of NIR optical transitions occurs at considerably larger overpotentials than one would expect from a simple model of shifting the Fermi level by the applied potential with the corresponding depletion/filing of Van Hove singularities. For instance, the $\upsilon_s^1 \rightarrow c_s^1$ transition (at 0.65 eV) should disappear at ±0.325 V vs the potential corresponding to the Fermi level. Figure 3 (in accord with previous reports on peapods[15] and empty SWCNT[4,16,24]) rather provides evidence that the $\upsilon_s^1 \rightarrow c_s^1$ transition remains active in a considerably broader potential window. Apparently, the double layer provides a smaller charge than required for the corresponding depletion/filling of singularities. This charge can be estimated from eq 1 to be only about 0.005 e^-/C atom for $\Delta U = 1$ V (cf. section 3.2).

In contrast to the previously studied empty SWCNT,[4] we do not detect shifts of these peaks upon progressive doping. This evidences that the peapod sample has a narrow distribution of tube diameters. (A polydisperse mixture of tubes would exhibit, upon doping, a blue shift of vis-NIR peaks.[4,20]) This conclusion is also supported by Raman spectra in the RBM region (see section 3.3.). A new peak, red-shifted by ca. 0.05 eV vs the $\upsilon_s^2 \rightarrow c_s^2$ transition, can be traced at anodic potentials around 1.7 V (Figure 3). This can be assigned to "doping-induced transition" occurring within the partly filled valence band ($\upsilon_s^n \rightarrow \upsilon_s^1$, $\upsilon_s^n \rightarrow \upsilon_s^2$) $n \geq 3$).[4,17,26]

3.3. Raman Spectroscopy. Figure 4 panels A and B show the Raman spectra of C_{60}@SWCNT and C_{70}@SWCNT, respectively. For comparison, spectra of the parent SWCNTs are also displayed. The radial-breathing mode (RBM) occurs between 165 and 185 cm^{-1} for C_{60}@SWCNT (Figure 4A) and between 160 and 180 cm^{-1} for C_{70}@SWCNT (Figure 4B). The diameter of peapods (d) is known to scale with the RBM frequency (ω):[10,21]

$$d \approx k/\omega \qquad (2)$$

The constant k (for ω in reciprocal centimeters and d in nanometers) was reported to range from 224 to 248 for SWCNT.[10,21,27,28] Equation 2 yields d between 1.2 and 1.5 nm for ω between 185 and 160 cm^{-1}, which is close to the diameters estimated from vis-NIR spectra (section 3.2). The RBM frequencies of C_{70}@SWCNT are slightly red-shifted, which provides evidence that the diameter of C_{70}@SWCNT is larger (cf. eq 2). This is in accord with the discussion of vis-NIR

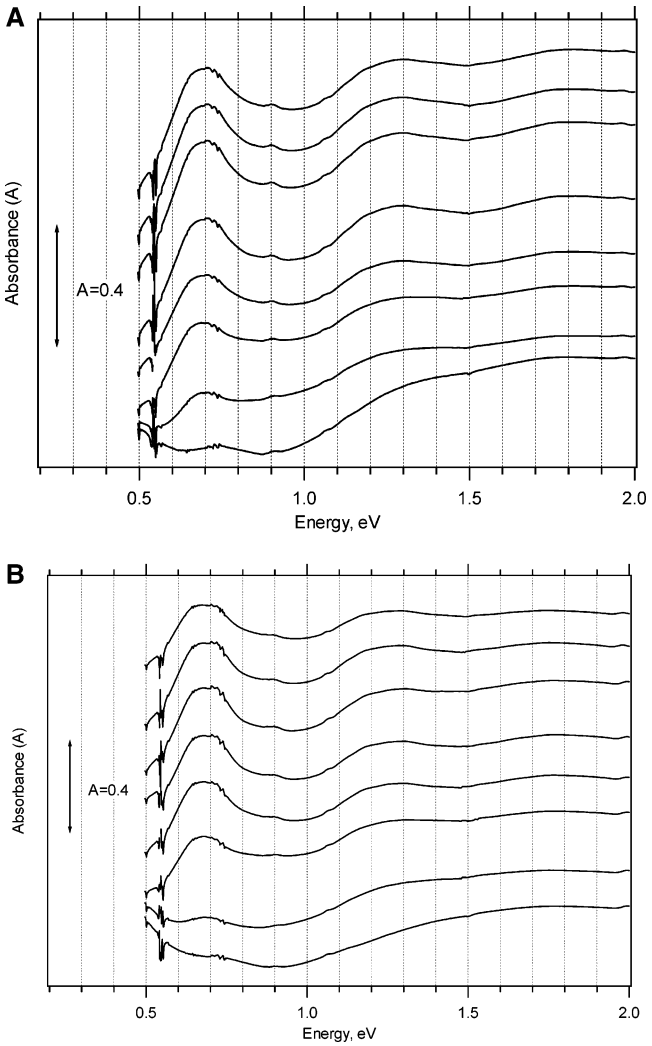

Figure 3. (A) Potential-dependent vis-NIR spectra of C_{60}@SWCNT peapods deposited on ITO electrode in 0.2 M $LiClO_4$ + acetonitrile. The applied potential varied by 0.3 V from −0.88 to 1.22 V vs Fc/Fc^+ for curves from top to bottom. Spectra are offset for clarity, but the absorbance scale is identical for all spectra (see scale bar). (B) Potential-dependent vis-NIR spectra of C_{70}@SWCNT peapods deposited on ITO electrode in 0.2 M $LiClO_4$ + acetonitrile. The applied potential varied by 0.3 V from −0.84 to 1.26 V vs Fc/Fc^+ for curves from top to bottom. Spectra are offset for clarity, but the absorbance scale is identical for all spectra (see scale bar).

spectra (section 3.2. and Figure 2). The expected diameter increase (red shift of RBM) of peapods vs empty tubes seems to be traced in Figure 4, although not that clearly. The red shift of RBM frequency in peapods was also mentioned previously.[8] (Note, however, that there is some mismatch in ref 8 and in the cross-cited ref 10.) Our Raman spectra confirm reasonable monodispersity of samples, which are free from narrow tubes, unable to accommodate C_{60}/C_{70}. In terms of the zone-folding.[19,20,26] the photons of 2.41 or 2.54 eV resonate with the transition ($\upsilon_s^3 \rightarrow c_s^3$) in tubes of diameters 1.2−1.5 nm.

As expected,[7,10] we can trace all the significant Raman lines of bare fullerenes in our peapods. The C_{60} peaks, marked by arrows in Figure 4A, can be assigned as follows: 270 cm^{-1}, $H_g(1)$; 430 cm^{-1}, $H_g(2)$; 494 cm^{-1}, $A_g(1)$; 709 cm^{-1}, $H_g(3)$; 769 cm^{-1}, $H_g(4)$; 1424 cm^{-1}, $H_g(7)$; 1465 cm^{-1}, $A_g(2)$. Both $A_g(1)$ and $A_g(2)$ modes show a distinguished satellite line at larger frequency (see also ref 10), which is difficult to interpret as the A_g modes are nondegenerate. Moreover, the splitting of A_g modes does not seem to be reproduced in the H_g modes.[10] The main line of pentagonal pinch mode, $A_g(2)$, occurs at 1465 cm^{-1}, i.e., it is downshifted by about 4 cm^{-1} vs that of free C_{60} (cf. also refs 7 and 10). This mode is known to soften by about 6 cm^{-1} per electron per C_{60} cage,[10,12] which would indicate partial electron transfer from SWCNT to C_{60}. However, the $A_g(2)$ satellite occurs at 1474 cm^{-1}, i.e., above the position of $A_g(2)$ in free C_{60} (1469 cm^{-1}).

Arrows in Figure 4B point to 11 intense C_{70} lines, which can be observed also in bare C_{70}. Their tentative assignment is as follows:[13,14] 260 cm^{-1} (A_1', E_2'); 450 cm^{-1} (A_1', E_1''); 563 cm^{-1} (A_1', E_1''); 699 cm^{-1} (A_1', E_1'', E_2'); 740 cm^{-1} (A_1', E_1'', E_2'); 1061 cm^{-1} (A_1', E_2'); 1181 cm^{-1} (A_1', E_1'', E_2'); 1226 cm^{-1} (A_1', E_1'', E_2'); 1256 cm^{-1} (E_1'', E_2'); 1443 cm^{-1} (A_1', E_1'', E_2'); 1466 cm^{-1} (A_1', E_1''). Also in the case of C_{70}@SWCNT, we can see significant splitting of some C_{70} lines, which is not reproduced in the bare C_{70} molecule. The most pronounced splitting occurs with lines at 260, 450, and 699 cm^{-1}.

In situ Raman spectra of electrochemically charged C_{60}@SWCNT excited at 2.41 or 2.54 eV are shown in Figure 5 panels A and B, respectively. In general, these spectra are well comparable to those reported in our previous short communication,[15] although the cited work did not present all spectral features shown in Figure 5, and also the sample used in our precedent work[15] was not of the same quality (its filling ratio was only ca. 60%). The intensities of RBM and TM decrease as a result of both cathodic and anodic charging. The maximum intensity is traced between ca. −0.6 and −0.3 V vs Fc/Fc^+, i.e., around the open circuit potential. Also the vis-NIR intensities have maximum values in this potential region (see section 3.2). The symmetric potential-controlled tuning of the RBM/TM intensities was reported previously for empty SWCNT.[4,24] In accord with these results,[4,24] the higher-frequency RBMs (at ca. 180−190 cm^{-1}) are less affected, compared to the low-frequency RBMs (at ca. 165−175 cm^{-1}). This is due to the diameter-selective transition energies.[19,20,26] Consequently, the υ_s^3/c_s^3 states of wide tubes are depleted/filled before those of narrower tubes, when the potential is changed toward more positive/negative values. A strong reductive doping with potassium caused the drop of RBM intensity by a factor of 100 (ref 10). Sood and co-workers[29] have recently discussed the RBM intensity vs electrochemical potential in terms of the changes in energy gaps between the Van Hove singularities.

In analogy to empty tubes,[4] the frequency of TM band significantly and monotonically upshifts with increasing anodic potential but it is less sensitive to cathodic charging (Figure 5). Stiffening of the graphene mode occurs if holes are introduced into the π band. The anodic frequency upshift per hole, $\Delta\omega/\Delta f$ (for estimation of Δf see eq 1), equals 460 cm^{-1} for graphite[30] and 250−320 cm^{-1} for SWCNT.[4,31] However, the $\Delta\omega/\Delta f$ ratios were much higher than expected for $\Delta U > 1.2$ V, presumably because of irreversible oxidation of the tubes.[4,24,30,31] Oxidative breakdown of peapods manifested itself by a spot "burning" after prolonged exposure of anodically polarized electrode to the laser light. A simultaneous application of the laser light and anodic polarization is essential for burning of peapods: no breakdown occurred (i) at the areas outside the laser spot of a polarized electrode and (ii) by laser excitation of an electrode at less positive potentials. The effects upon cathodic charging are more complex. Electrochemical[4,9,32] or chemical[33,34] reductive doping of SWCNTs causes the TM frequency upshifts or downshifts depending on the counterion used (Li^+, K^+, Rb^+) and the doping level, but the interpretation of such effects is not yet fully consistent.[9,32−34]

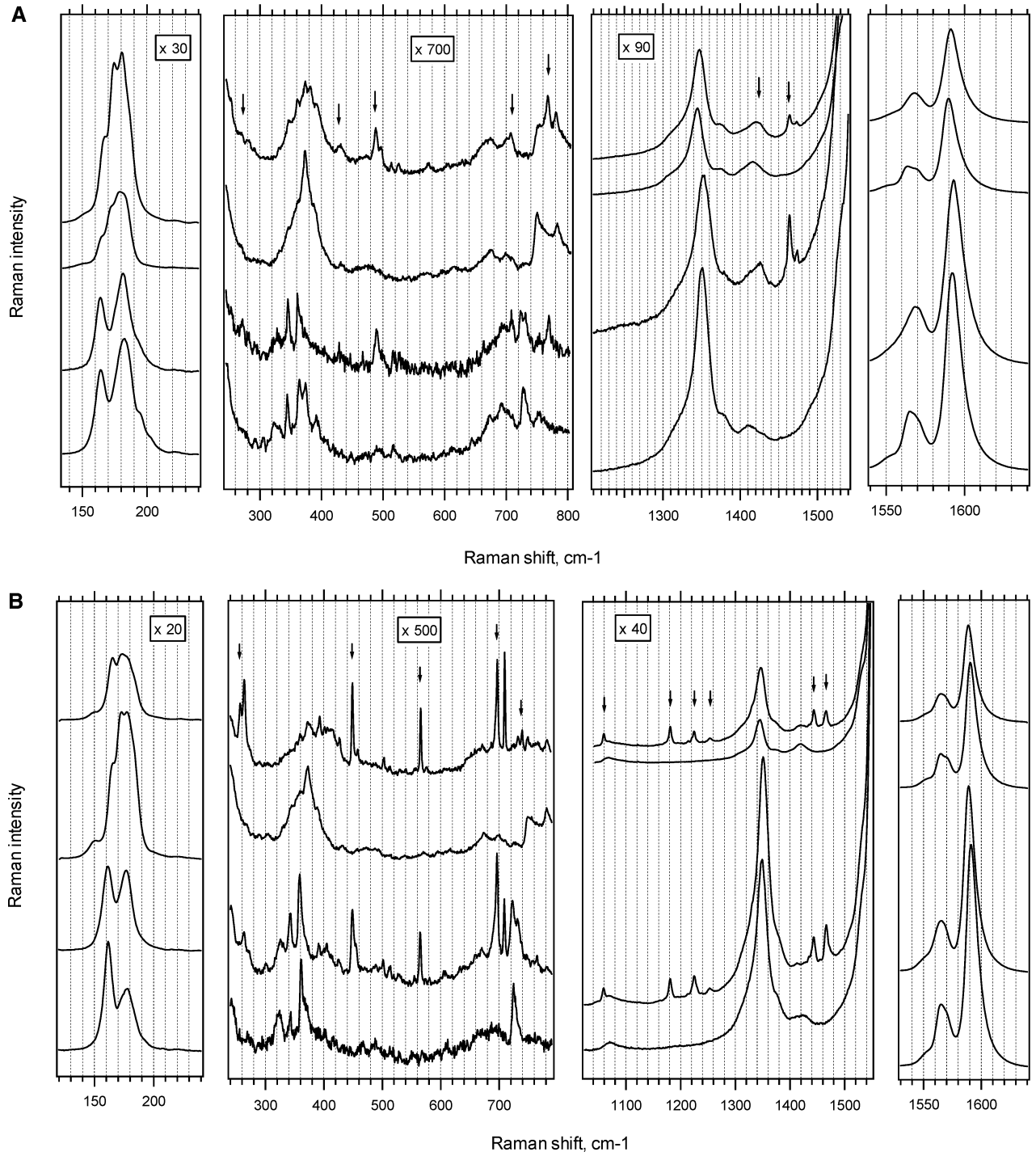

Figure 4. (A) Raman spectra of C_{60}@SWCNT (peapods) and the corresponding parent empty tubes (SWCNT). The spectra were recorded with dry samples in the form of buckypaper. From top to bottom: C_{60}@SWCNT (excitation 2.41 eV), SWCNT (excitation 2.41 eV), C_{60}@SWCNT (excitation 2.54 eV), and SWCNT (excitation 2.54 eV). Arrows indicate the expected Raman lines of C_{60}. Spectra are offset for clarity and zoomed in the first three windows as indicated. The intensity scale was normalized vs the intensity of F_{1g} mode of Si at 520.2 cm^{-1}. (B) Raman spectra of C_{70}@SWCNT (peapods) and the corresponding parent empty tubes (SWCNT). The spectra were recorded with dry samples in the form of buckypaper. From top to bottom: C_{70}@SWCNT (excitation 2.41 eV), SWCNT (excitation 2.41 eV), C_{70}@SWCNT (excitation 2.54 eV), and SWCNT (excitation 2.54 eV). Arrows indicate the expected Raman lines of C_{70}. Spectra are offset for clarity and zoomed in the first three windows as indicated. The intensity scale was normalized vs the intensity of F_{1g} mode of Si at 520.2 cm^{-1}.

Cathodic doping of C_{60}@SWCNT causes overall decrease of intensities, while the C_{60} lines drop below a detectable level (Figure 5). This matches qualitatively the behavior upon K-doping.[10] An interesting effect is observed upon progressive anodic doping, which is difficult to follow chemically. Figure 5 displays a significant increase of Raman intensities of C_{60} modes. The "anodic enhancement" is apparent for all C_{60}-related modes, except the satellite lines of $A_g(1)$ and $A_g(2)$ modes at 500 and 1474 cm^{-1}, respectively. As the tube-related modes decline monotonically upon both cathodic and anodic doping (see above), the fullerene-related mode $A_g(2)$ becomes dominant over the tube-related modes (the D mode at ca. 1350 cm^{-1} and RBM) at positive potentials. Another effect of anodic charging consist in the gradual disclosure of $H_g(8)$ line at ca. 1573 cm^{-1} enabled by the upshift of the TM mode. This mode is normally hidden in strong tube-related features and cannot be observed

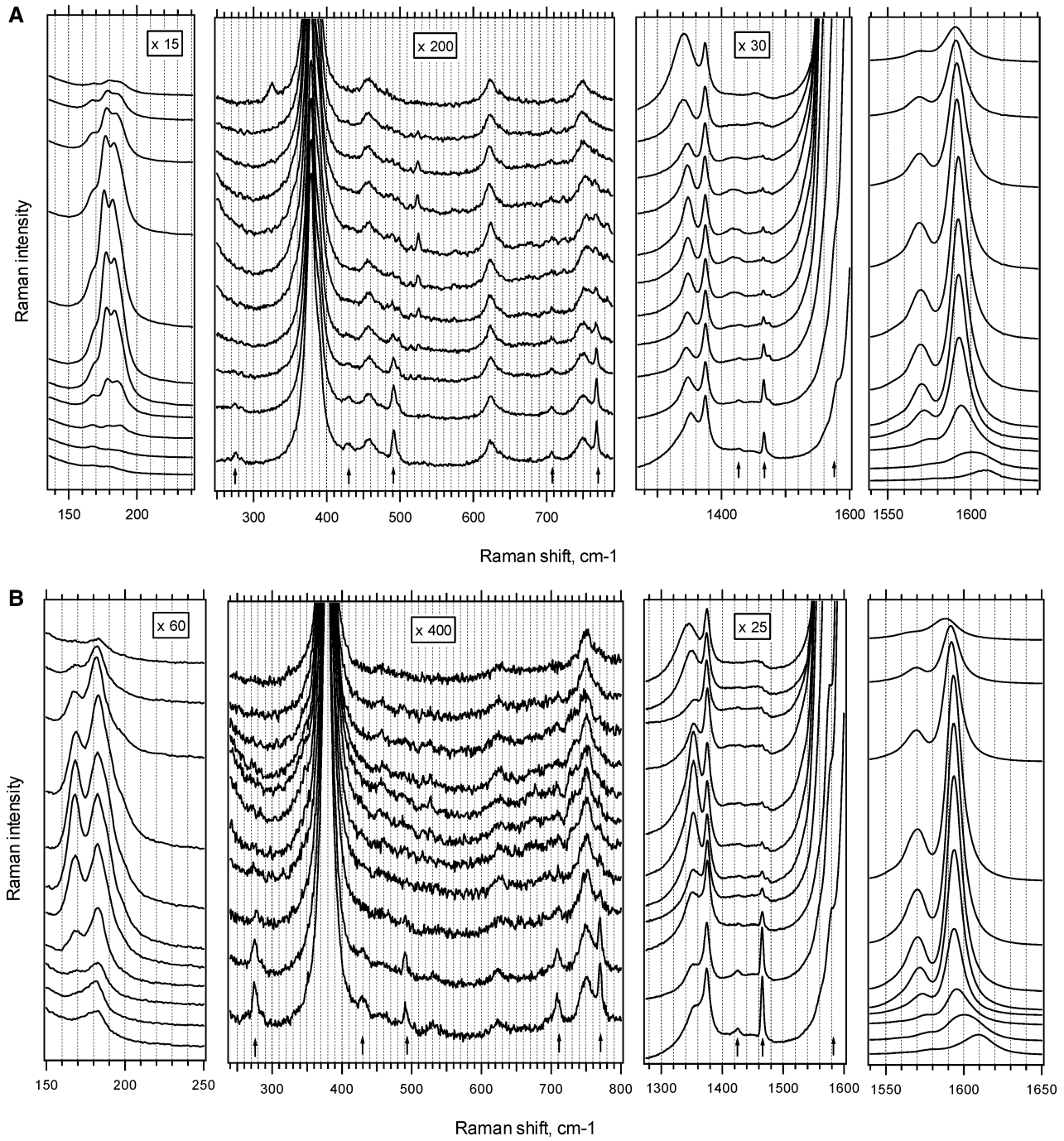

Figure 5. (A) Potential-dependent Raman spectra of C_{60}@SWCNT (peapods) on Pt electrode (excited at 2.41 eV) in 0.2 M $LiClO_4$ + acetonitrile. The electrode potential varied by 0.3 V from −1.75 to 1.25 V vs Fc/Fc^+ for curves from top to bottom. Spectra are offset for clarity, but the intensity scale is identical for all spectra in the respective window. The intensities are zoomed in the first three windows as indicated. Arrows indicate the expected Raman lines of C_{60}. The peaks at 378.5 and 1374.5 cm^{-1} belong to acetonitrile. (B) Potential-dependent Raman spectra of C_{60}@SWCNT (peapods) on Pt electrode (excited at 2.54 eV) in 0.2 M $LiClO_4$ + acetonitrile. The electrode potential varied by 0.3 V from −1.73 to 1.27 V vs Fc/Fc^+ for curves from top to bottom. Spectra are offset for clarity, but the intensity scale is identical for all spectra in the respective window. The intensities are zoomed in the first three windows as indicated. Arrows indicate the expected Raman lines of C_{60}. The peaks at 378.5 and 1374.5 cm^{-1} belong to acetonitrile.

in dry peapods without electrochemical charging. We should also mention two interesting Raman bands at 515 and 525 cm^{-1}, which are specific for C_{60}@SWCNT only (they are missing in empty tubes, Figure 4A) but which show the symmetric charging response as the RBM/TM bands (Figure 5A,B).

The enhancement of the intensity of C_{60}-related Raman modes is a specific feature of C_{60}@SWCNT. The $A_g(2)$ mode in a solid C_{60} film drops considerably along with frequency downshift upon cathodic reduction (data not shown here). The doping of C_{60} with potassium vapor toward KC_{60}, K_3C_{60}, K_4C_{60}, and K_6C_{60} is accompanied by the same effect.[12] On the other hand, fullerene C_{60} is known to be idle toward oxidation even at high anodic potentials. The $A_g(2)$ line in peapods shows no frequency shift upon electrochemical doping (Figures 4A and 5A,B), compared to its position in pristine peapods (1465 cm^{-1}). This demonstrates, as expected, (i) no transfer of holes from the nanotubes to the C_{60} and (ii) no dimerization or photodecomposition of C_{60} under the experimental conditions used. (The $C_{60}-C_{60}$ reactions would cause softening of the $A_g(2)$ mode by ca. 10 cm^{-1}.[35]) Whereas the quenching of SWCNT-related

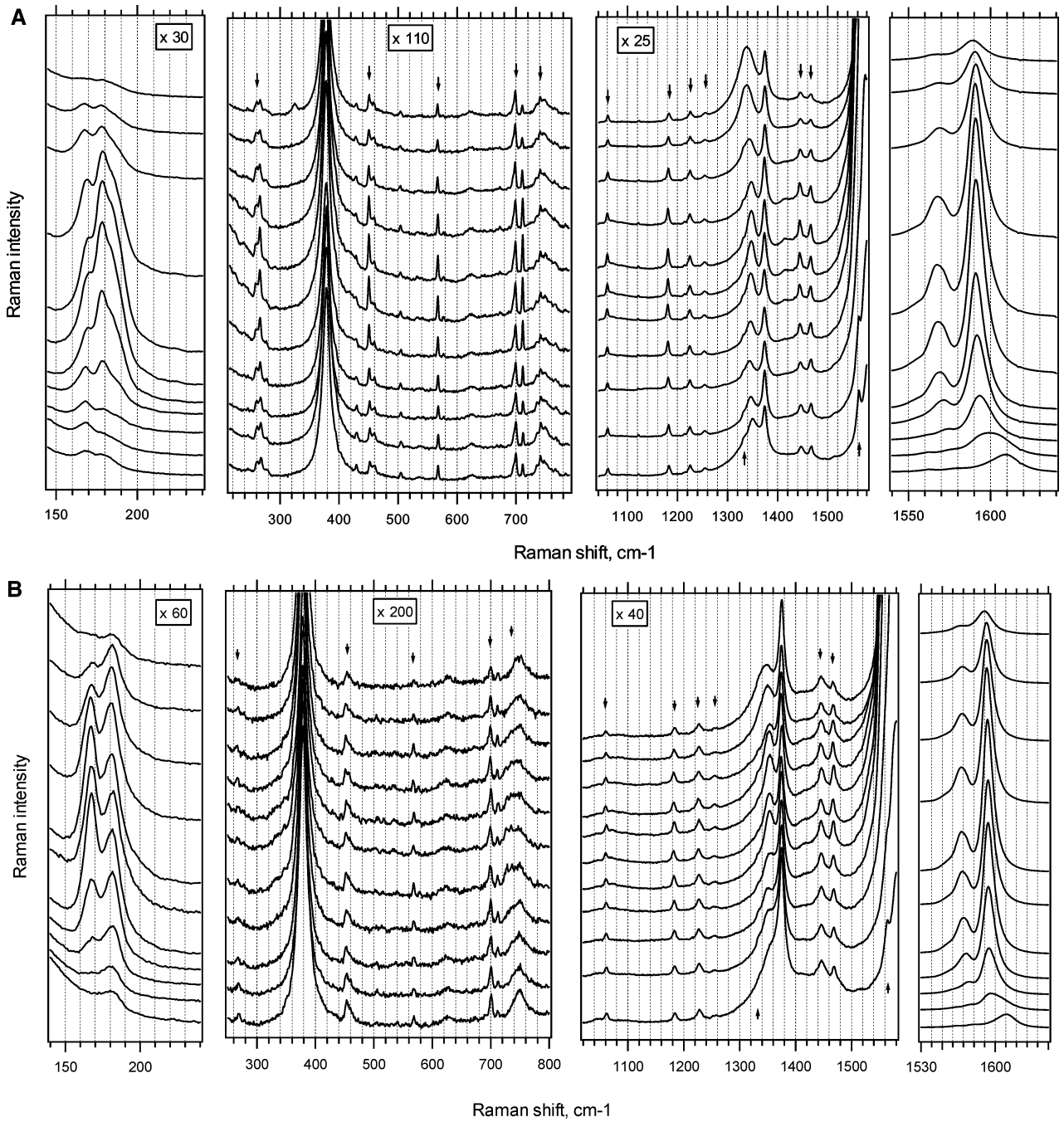

Figure 6. (A) Potential-dependent Raman spectra of C_{70}@SWCNT (peapods) on Pt electrode (excited at 2.41 eV) in 0.2 M $LiClO_4$ + acetonitrile. The electrode potential varied by 0.3 V from −1.79 to 1.21 V vs Fc/Fc^+ for curves from top to bottom. Spectra are offset for clarity, but the intensity scale is identical for all spectra in the respective window. The intensities are zoomed in the first three windows as indicated. Arrows indicate the expected Raman lines of C_{70}. The peaks at 378.5 and 1374.5 cm^{-1} belong to acetonitrile. (B) Potential-dependent Raman spectra of C_{70}@SWCNT (peapods) on Pt electrode (excited at 2.54 eV) in 0.2 M $LiClO_4$ + acetonitrile. The electrode potential varied by 0.3 V from −1.76 to 1.24 V vs Fc/Fc^+ for curves from top to bottom. Spectra are offset for clarity, but the intensity scale is identical for all spectra in the respective window. The intensities are zoomed in the first three windows as indicated. Arrows indicate the expected Raman lines of C_{70}. The peaks at 378.5 and 1374.5 cm^{-1} belong to acetonitrile.

modes is symmetrical in terms of depletion/filling of the spike states around the Fermi level, the electrochemical charging of C_{60} is inherently possible in the cathodic direction only (up to C_{60}^{6-}).[1] Nevertheless, the resistance of C_{60} toward oxidation does not seem to be a key for interpreting of the unusual anodic enhancement of Raman intensities, because the C_{60} peapods are screened by the peapod wall (see section 3.4 for further discussion).

Surprisingly, the Raman spectroelectrochemistry of C_{70}@SWCNT demonstrates qualitatively different behavior as compared to that of C_{60}@SWCNT. The most striking feature is the absence of "anodic enhancement" (observed in C_{60}@SWCNT, vide ultra) (Figure 6). The relevant Raman modes of C_{70} peas show the "normal" symmetric potential dependence (as the RBM/TM lines), although not all the peapod-specific bands show the same sensitivity to charging. This is especially expressed with doublet lines at 699/705 and 450/460 cm^{-1} (Figure 6). As in the case of C_{60}@SWCNT, electrochemical charging allows detecting of some lines, which are normally hidden by overlapping D and G lines of SWCNT: 1332 and 1564 cm^{-1} respectively (tentative assignment E_2' and E_1', respectively). The latter line is the strongest line in Raman

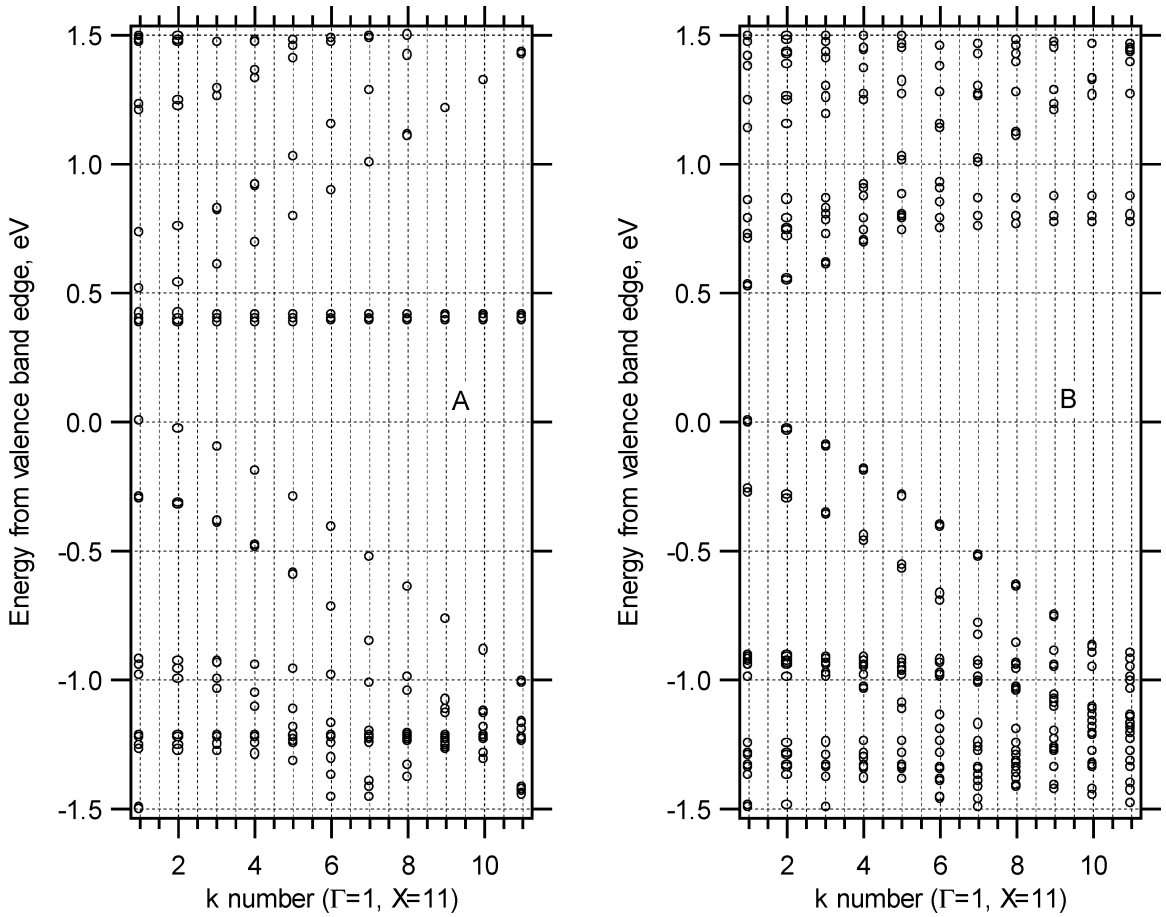

Figure 7. Calculated band structure of (A) C_{60}@SWCNT(17,0) and (B) standing C_{70}@SWCNT(17,0).

spectrum of bare C_{70}, which is, however, not detectable in peapods because of its overlap with TM.

3.4. Theoretical Model and Interpretation of Experimental Data. To interpret the nonsymmetric anodic enhancement of Raman intensities in C_{60}@SWCNT, we suggest the following hypothesis: Electrochemical charge interacts primarily with the peapod wall only, causing the depletion/filling of states close to the Fermi level of the wall (SWCNT). This manifests itself by symmetric anodic/cathodic bleaching of the RBM/TM intensities and frequency shifts of TM. The asymmetric potential response of C_{60} peas is caused by the fact that the position of the Fermi level of SWCNT is close to the LUMO of C_{60} (t_{1u}).[23] This anomalous drop of the LUMO band is due to the hybridization of the nearly free electron state of SWCNT and the π-state of C_{60}, which depends only on the diameter but not on the chirality of SWCNT.[23]

For cathodic polarization, electrons may be transferred from the wall to the LUMO band of C_{60} peas. Thus, the HOMO−LUMO transition is efficiently suppressed by cathodic doping of the wall, and the resonance Raman scattering of C_{60} is quenched as in the case of SWCNT modes. On the other hand, the anodic depletion of the valence band of SWCNT has no influence on the electronic transitions of C_{60} peapods. Consequently, the HOMO−LUMO transfer in C_{60} peapods is allowed at potentials above the Fermi level. At the same time, the SWCNT-related transitions are suppressed by depletion of the valence band, and the wall becomes optically "better transparent" for the exiting photons.

To get further insight into this problem, we have calculated two model systems, in which SWCNT(17,0) was filled either with C_{60} or with standing C_{70}. All calculations have been performed with the local-density approximation in the density functional theory.[36,37] For the exchange-correlation energy among electrons, a functional form[38] was fitted to the Monte Carlo results for the homogeneous electron gas.[39] Norm-conserving pseudopotentials were adopted to describe the electron−ion interaction.[40,41] In constructing the pseudopotentials, core radii adopted for C 2s and 2p states are both 1.5 Bohrs. The valence wave functions were expanded by the plane-wave basis set with a cutoff energy of 50 Ry. A supercell model was adopted, in which a peapod is placed with its nanotube wall being separated by 7 Å from another wall of an adjacent peapod. The conjugate-gradient minimization scheme was utilized both for the electronic structure calculation and for the geometry optimization. In the geometry optimization, commensurability condition was imposed between the one-dimensional periodicity of the atomic arrangements in the nanotube and that of the chain of fullerenes. Integration over one-dimensional Brillouin zone was carried out with two k points.

Figure 7 displays the results. In the case of standing C_{70}, the LUMO is located above the conduction band of SWCNT. For C_{60}, the LUMO is located in the band gap of SWCNT. The standing fullerene C_{70} in SWCNT(17,0) keeps the LUMO position higher compared to that of C_{60} in SWCNT(17,0). Cathodic charging of C_{60}@SWCNT (peapods) causes the extra electrons to interact efficiently with the C_{60} and the HOMO−LUMO transition is quenched.

Since the potential-dependent Raman intensities of C_{70} in C_{70}@SWCNT copy mostly the corresponding Raman intensities of RBM/TM of the wall, the electronic interactions of C_{70} with the wall are more significant than in the case of C_{60} peapods. This might be interpreted by assuming a smaller HOMO−

LUMO gap in C_{70} and a larger number of allowed electronic transitions in C_{70}, which are also strongly and more extensively coupled to the vibrational states.[13,14] The complex electronic structure of C_{70} causes both components to respond similarly to external charging. In other words, the system with the larger number of allowed electronic transitions (C_{70}@SWCNT) is also more sensitive to electrochemical perturbations of these transitions. The absence of "anodic enhancement" in C_{70}@SWCNT indicates that the electrochemical p-doping of the wall is efficiently coupled to the electronic transitions of C_{70}, even though both C_{60} and C_{70} show virtually identical electrochemistry in the form of free molecules.[1]

The fact that the electronic interaction of C_{70} with the wall is more intimate than that of C_{60} can be illustrated also by a simple geometric argument based on the possibility of different C_{70} orientations against the SWCNT wall.[7] As the parent SWCNTs have some diameter distribution, the intratubular fullerenes are also accommodated in tubes of varying diameters. The array of peapod diameters is obviously dictated by the size of the particular fullerene, which requires also some distance from the wall. If this distance increases, the fullerene LUMO band drops, and this allows the C_{60} LUMO can shift to a position near the Fermi level.[23] For nonspherical fullerenes, like C_{70}, the LUMO drop can be compensated by the reorientation of intratubular C_{70} molecules from "lying" to "standing" positions, while the optimum C_{70}−wall distance is again restored. This steric compensation is inherently excluded for C_{60} because of its spherical symmetry. The "thick" C_{60} peapods have their LUMO band near the Fermi level, while it can even be partly filled and the Raman resonance is partly quenched. Anodic charging of thick C_{60} peapods will deplete the half-filled LUMO, which efficiently enhances the overall Raman intensity of intratubular C_{60}.

Future efforts should be aimed at spectroelectrochemical investigations and detailed assignment of Raman spectra of peapods with higher fullerenes (such as C_{76}, C_{78}, and C_{84}; cf. ref 21) to decide whether the "anodic enhancement" is an exclusive feature of C_{60}@SWCNT.

4. Conclusions

Charge transfer on fullerene peapods (C_{60}@SWCNT and C_{70}@SWCNT) was studied electrochemically in 0.2 M $LiClO_4$ + acetonitrile. The reduction of intratubular fullerene (C_{60} or C_{70}) is hampered; hence, no fullerene-related faradaic processes are detectable. Electrochemistry of peapods is dominated by capacitive double-layer charging, analogous to that of empty SWCNT.

Vis-NIR spectroelectrochemistry traces mostly the effects occurring in the peapod wall (SWCNT). Electrochemical charging leads to reversible and fast bleaching of the electronic transitions between Van Hove singularities. This also causes reversible quenching of resonance Raman scattering of both radial breathing and tangential modes of the SWCNT wall.[24] The quenching of Raman intensities of the tube-related modes is potential-symmetric and is accompanied by the corresponding frequency shifts.

In both types of peapods, the charging-induced frequency shifts allow detecting of some lines of intratubular fullerenes, which are normally hidden by overlapping tangential modes of SWCNT. The C_{60}-related Raman modes of C_{60}@SWCNT (peapods) decrease intensity at cathodic potentials but increase considerably at anodic potentials. On the contrary, the relevant Raman modes of C_{70} in C_{70}@SWCNT (peapods) show the "normal" potential-symmetric bleaching, analogous that of the tube-related modes.

On the basis of model calculations of SWCNT(17,0) filled with either C_{60} or standing C_{70}, the observed effects were interpreted in terms of the specific electronic structure of C_{60}@SWCNT (peapods). The key argument is that the optical HOMO−LUMO transitions of intratubular fullerenes (C_{60} or C_{70}) show different sensitivity toward electrochemical perturbations. The LUMO of C_{60} (t_{1u}) is unusually close to the Fermi level of C_{60}@SWCNT (peapod), while it may even drop into the conduction band, if the C_{60} is accommodated in sufficiently wide SWCNT. This is excluded in C_{70}@SWCNT (peapods), where the LUMO occurs always at relatively higher energies. Even in wide C_{70}@SWCNT (peapods) the higher LUMO position is kept via structural reorientation of intratubular C_{70} from "lying" into the "standing" positions. This explains the observed Raman intensities of electrochemically doped peapods in general and the "anodic Raman enhancement" of C_{60}@SWCNT (peapods) in particular.

Acknowledgment. This work was supported by IFW Dresden, by the Academy of Sciences of the Czech Republic (Contract A4040306), and by the Czech Ministry of Education (CZ-JP Cooperation Grant ME487).

References and Notes

(1) Xie, Q.; Perez-Codero, E.; Echegoyen, L. *J. Am. Chem. Soc.* **1992**, *114*, 3978.

(2) Jehoulet, C.; Obeng, Y. O.; Kim, Y. T.; Zhou, F.; Bard, A. J. *J. Am. Chem. Soc.* **1992**, *114*, 4237.

(3) Janda, P.; Krieg, T.; Dunsch, L. *Adv. Mater.* **1998**, *17*, 1434.

(4) Kavan, L.; Rapta, P.; Dunsch, L.; Bronikowski, M. J.; Willis, P.; Smalley, R. E. *J. Phys. Chem. B* **2001**, *105*, 10764.

(5) Frackowiak, E.; Beguin, F. *Carbon* **2001**, *39*, 937.

(6) Smith, B. W.; Monthioux, M.; Luzzi, D. E. *Nature* **1998**, *396*, 323.

(7) Kataura, H.; Maniwa, Y.; Abe, M.; Fujiwara, A.; Kodama, T.; Kikuchi, K.; Imohori, H.; Misaki, Y.; Suzuki, S.; Achiba, Y. *Appl. Phys. A* **2002**, *74*, 349.

(8) Liu, X.; Pichler, T.; Knupfer, M.; Golden, M. S.; Fink, J.; Kataura, H.; Achiba, Y.; Hirahara, K.; Iijima, S. *Phys. Rev. B* **2002**, *65*, 045419.

(9) Claye, A.; Rahman, S.; Fischer, J. E.; Sirenko, A.; Sumanasekera, G. U.; Eklund, P. C. *Chem. Phys. Lett.* **2001**, *333*, 16.

(10) Pichler, T.; Kuzmany, H.; Kataura, H.; Achiba, Y. *Phys. Rev. Lett.* **2001**, *87*, 267401.

(11) Kataura, H.; Maniwa, Y.; Kodama, T.; Kikuchi, K.; Hirahara, K.; Suenaga, K.; Iijima, S.; Suzuki, S.; Achiba, Y.; Kratschmer, W. *Synth. Metals* **2001**, *121*, 1195.

(12) Kuzmany, H.; Matus, M.; Burger, B.; Winter, J. *Adv. Mater.* **1994**, *6*, 731.

(13) Schettino, V.; Pagliai, M.; Cardini, G. *J. Phys. Chem. A* **2002**, *106*, 1815.

(14) Gallagher, S. H.; Armstrong, R. S.; Bolskar, R. D.; Lay, P. A.; Reed, C. A. *J. Am. Chem. Soc.* **2002**, *119*, 4263.

(15) Kavan, L.; Dunsch, L.; Kataura, H. *Chem. Phys. Lett.* **2002**, *361*, 79.

(16) Kazaoui, S.; Minami, N.; Matsuda, N.; Kataura, H.; Achiba, Y. *Appl. Phys. Lett.* **2001**, *78*, 3433.

(17) Kazaoui, S.; Minami, N.; Jacquemin, R.; Kataura, H.; Achiba, Y. *Phys. Rev. B* **1999**, *60*, 13339.

(18) Petit, P.; Mathis, C.; Journet, C.; Bernier, P. *Chem. Phys. Lett.* **1999**, *305*, 370.

(19) Alvarez, L.; Righi, A.; Guillard, T.; Rols, S.; Anglaret, E.; Laplaze, D.; Sauvajol, J. L. *Chem. Phys. Lett.* **2000**, *316*, 186.

(20) Kataura, H.; Kumazawa, Y.; Maniwa, Y.; Umezu, I.; Suzuki, S.; Ohtsuka, Y.; Achiba, Y. *Synth. Metals* **1999**, *103*, 2555.

(21) Bandow, S.; Takizawa, M.; Kato, H.; Okazaki, T.; Shinohara, H.; Iijima, S. *Chem. Phys. Lett.* **2001**, *347*, 23.

(22) Luzzi, D. E.; Smith, B. W. *Carbon* **2000**, *38*, 1751.

(23) Okada, S.; Saito, S.; Oshiyama, S. *Phys. Rev. Lett.* **2001**, *86*, 3835.

(24) Kavan, L.; Rapta, P.; Dunsch, L. *Chem. Phys. Lett.* **2000**, *328*, 363.

(25) Kazaoui, S.; Minami, N.; Kataura, H.; Achiba, Y. *Synth. Metals* **2001**, *121*, 1201.

(26) Jacquemin, R.; Kazaoui, S.; Yu, D.; Hassanien, A.; Minami, N.; Kataura, H.; Achiba, Y. *Synth. Metals* **2000**, *115*, 283.

(27) Bandow, S.; Asaka, S.; Saito, Y.; Rao, A. M.; Grigorian, L.; Richter, E.; Eklund, P. C. *Phys. Rev. Lett.* **1998**, *80*, 3779.
(28) Jorio, A.; Saito, R.; Hafner, J. H.; Lieber, C. M.; Hunter, M.; McClure, T.; Dresselhaus, G.; Dresselhaus, M. S. *Phys. Rev. Lett.* **2001**, *86*, 118.
(29) Ghosh, S.; Sood, A. K.; Rao, C. N. R. *J. Appl. Phys.* **2002**, *92*, 1165.
(30) Rao, A. M.; Eklund, P. C.; Bandow, S.; Thess, A.; Smalley, R. E. *Nature* **1997**, *388*, 257.
(31) Sumanasekera, G. U.; Allen, J. L.; Fang, S. L.; Loper, A. L.; Rao, A. M.; Eklund, P. C. *J. Phys. Chem. B* **1999**, *103*, 4292.
(32) Claye, A.; Nemes, N. M.; Janossy, A.; Fischer, J. E. *Phys. Rev. B* **2000**, *62*, R4845−R4848.
(33) Bendiab, N.; Anglaret, E.; Bantignies, J. L.; Zahab, A.; Sauvajol, J. L.; Petit, P.; Mathis, C. *Phys. Rev. B* **2001**, *64*, 245424.
(34) Bendiab, N.; Spina, L.; Zahab, A.; Poncharal, P.; Marliere, C.; Bantignies, J. L.; Anglaret, E.; Sauvajol, J. L. *Phys. Rev. B* **2001**, *63*, 153407.
(35) Bandow, S.; Takizawa, M.; Hirahara, K.; Yudasaka, M.; Iijima, S. *Chem. Phys. Lett.* **2001**, *337*, 48.
(36) Hohenberg, P.; Kohn, W. *Phys. Rev. B* **1964**, *136*, 864.
(37) Kohn, W.; Sham, L. J. *Phys. Rev. A* **1965**, *140*, 1133.
(38) Perdew, J. P.; Zunger, A. *Phys. Rev. B* **1981**, *23*, 5048.
(39) Ceperley, D. M.; Alder, B. J. *Phys. Rev. Lett.* **1980**, *45*, 566.
(40) Troullier, N.; Martins, J. L. *Phys. Rev. B* **1991**, *43*, 1993.
(41) Kleinman, L.; Bylander, D. M. *Phys. Rev. Lett.* **1982**, *48*, 1425.